Fermi Arc Criterion for Surface Majorana Modes in Superconducting Time-Reversal Symmetric Weyl Semimetals

Rauf Giwa and Pavan Hosur

Phys. Rev. Lett. **127**, 187002 — Published 26 October 2021

DOI: 10.1103/PhysRevLett.127.187002

Fermi arc criterion for surface Majorana modes in superconducting time-reversal symmetric Weyl semimetals

Rauf Giwa, Pavan Hosur[1]

[1]*Department of Physics, University of Houston, Houston 77204, USA*

Many clever routes to Majorana fermions have been discovered by exploiting the interplay between superconductivity and band topology in metals and insulators. However, realizations in semimetals remain less explored. We ask, "under what conditions do superconductor vortices in time-reversal symmetric Weyl semimetals – three-dimensional semimetals with only time-reversal symmetry – trap Majorana fermions on the surface?" If each constant-k_z plane, where z is the vortex axis, contains equal numbers of Weyl nodes of each chirality, we predict a generically gapped vortex and derive a topological invariant $\nu = \pm 1$ in terms of the Fermi arc structure that signals the presence or absence of surface Majorana fermions. In contrast, if certain constant-k_z planes contain a net chirality of Weyl nodes, the vortex is gapless. We analytically calculate ν within a perturbative scheme and provide numerical support with a lattice model. The criteria survive the presence of other bulk and surface bands and yield phase transitions between trivial, gapless and topological vortices upon tilting the vortex. We propose Li($Fe_{0.91}Co_{0.09}$)As and $Fe_{1+y}Se_{0.45}Te_{0.55}$ with broken inversion symmetry as candidates for realizing our proposals.

The interplay of band topology and superconductivity has paved new routes to Majorana fermions (MFs) – as topologically protected zero energy bound states trapped in topological defects such as superconductor vortices [1–20]. Following realizations in semiconductor nanowire-superconductor heterostructures [11, 14, 21], MFs were recently found for the first time in a three-dimensional (3D) system – at the ends of vortices in the bulk superconductor $FeSe_{0.45}Te_{0.55}$ [22–26]. This inspires a fundamental question: in a 3D superconductor, what properties of the normal state band structure ensure that vortices trap protected MFs at their ends? Restricting to bands with time-reversal symmetry ($\mathcal{T}$), since $\mathcal{T}$ enables a Cooper instability to begin with, sufficient conditions are known in two generic cases: a band insulator (metal) yields MFs if it is topological [5] (a modestly doped topological insulator [6]).

The third type of generic $\mathcal{T}$-preserving band material is a time-reversal symmetric Weyl semimetal (TWSM) [27–30]. Here, point intersections between non-degenerate bands create Weyl nodes (WNs) that possess a chirality of ± 1 and appear in quadruplets to respect $\mathcal{T}$ and Brillouin zone periodicity. Weyl semimetals constitute topological matter as they are immune to perturbations that do not hybridize anti-chiral WNs, i.e., WNs of opposite chirality and exhibit numerous topological responses [31–57]. On the surface, the bulk band topology manifests as Fermi arcs (FAs) that connect surface projections of anti-chiral WNs.

Motivated by the quest for MFs, we ask, "what is the fate of a superconductor vortex in a TWSM?" We show that there are three possible vortex phases – (i) gapped, with end-MFs; (ii) gapped, without end-MFs; (iii) gapless, with topologically protected chiral MFs dispersing along the vortex axis $\hat{\mathbf{z}}$. Crucially, we prove that the vortex phase relies solely on basic band structure data, namely, the FA configuration on the surface normal to $\hat{\mathbf{z}}$ and the locations of the bulk WNs. Remarkably, simply tilting the vortex can drive transitions between the three phases.

The criteria for the phases are as follows (see Fig. 1). Within each constant-k_z plane, identify the pair(s) of anti-chiral WNs that are closest to each other in periodic $\boldsymbol{k}$-space. Connect the partners with a geodesic and project it onto the surface. From the remaining WNs, identify the next closest pair(s) and project their geodesic(s) onto the surface, and so on for all WNs and constant-k_z planes. If all the WNs find partners in this process, the surface Brillouin zone will contain a set of lines that, along with the FAs, form closed *Fermi-geodesic loops*. In general, the surface will also carry closed Fermi loops and Dirac nodes. If the total number of Fermi-geodesic loops, Fermi loops and Dirac nodes is M, we predict a gapped vortex with a topological invariant

$$\nu = (-1)^M \tag{1}$$

Thus, odd M yields a topologically protected MF in the vortex core on the surface whereas even M does not. All WNs find partners only if each constant-k_z plane contains equal numbers of left- and right-handed WNs. For a minimal TWSM with four WNs at $(\pm\boldsymbol{K}_1, \pm\boldsymbol{K}_2)$, a vortex direction such that $|K_{1z}| = |K_{2z}|$ ensures this, while general TWSMs with more WNs need a mirror or glide symmetry plane parallel to $\hat{\mathbf{z}}$ – which is present in most TWSMs [45, 58–60] – to ensure all WNs are partnered. Generically, though, some WNs will lack partners and the surface will host open *Fermi-geodesic arcs* whose end-points will be projections of the unpartnered WNs. Each such WN will contribute a 1D chiral MF to the bulk vortex spectrum with a chirality equal to its own chirality times the vorticity of ± 1. The vortex will be in a gapless phase protected by k_z-conservation, analogous to the topological protection of a Weyl semimetal by 3D momentum conservation.

These criteria hold for general pairing symmetries provided the superconductor is gapped in the absence of a vortex. They survive doping around the WNs if the resulting Fermi surfaces are well-separated and the presence of trivial Fermi surfaces with rare exceptions. They are also im-

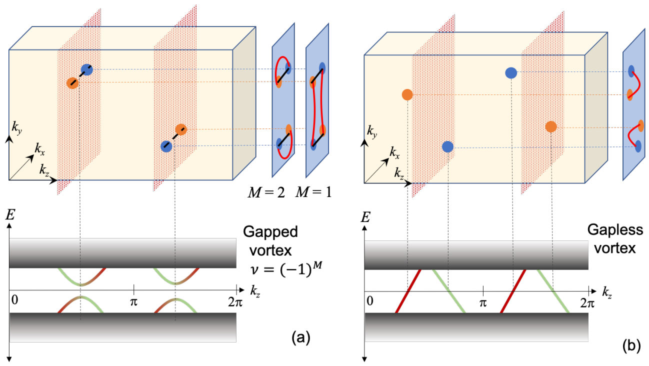

Figure 1. Schematic of the main result. Orange (blue) dots denote right(left)-handed WNs which produce right(left)-moving chiral MFs, colored red (green), inside the vortex. To determine the vortex phase, identify pairs of anti-chiral WNs at the same k_z and project the line joining them onto the surface. If these lines (solid black), along with the FAs (red curves), form M closed loops, the vortex is gapped and has a topological invariant $\nu = (-1)^M$ (a), whereas open arcs produce a gapless vortex (b).

mune to surface effects unless the surface is exposed to a topological insulator, in which case M effectively acquires the odd number of surface Fermi loops or Dirac nodes of the latter. Finally, (1) captures the known results for metals [6] and insulators [5], which lack Fermi-geodesic contours but may have Fermi loops and Dirac nodes.

Eq. (1) is obtained by computing the $\mathbb{Z}_2$ topological invariant for the vortex viewed as a 1D superconductor [7, 61, 62]. We require a mild assumption in the clean limit: for a given WN, if the two nearest anti-chiral WNs at the same k_z are at distances ΔK_1 and ΔK_2, then $e^{\frac{\hbar\xi}{\Delta_0}[v_1(\Delta K_1)^2 - v_2(\Delta K_2)^2]} \gg 1$ or $\Delta K_1 \gtrsim \Delta K_2$, where Δ_0 and ξ are superconducting properties – the uniform pairing amplitude and coherence length, respectively – and v_i is the typical Weyl velocity along ΔK_i. This condition ensures that the dominant hybridization is between chiral MFs from neighboring anti-chiral WNs, assuming hybridization is driven by band curvature. If hybridization is due to non-magnetic disorder that is smooth over distance ℓ_D, the requirement becomes $\Delta K_1 \gg \ell_D^{-1} \gg \Delta K_2$ while magnetic disorder invalidates (1). Disorder can be suppressed in principle whereas band curvature is unavoidable, so a physical regime of validity of (1) exists. We neglect hybridization between equi-chiral chiral MFs, i.e., chiral MFs of the same chirality, which amounts to smoothly deforming any accidentally gapless non-chiral vortex minibands away from zero energy.

Heuristically, (1) says that vortex-end MFs are present (absent) if the TWSM normal state is "closer" to a topological (trivial) insulator. To see this, imagine moving the WNs along the geodesics and annihilating them in pairs. If all WNs get annihilated, the resulting insulator will be topological (trivial) if the surface FAs evolve into an odd (even) number of surface Fermi loops, while the vortex will be topological (trivial). However, the vortex spectrum remains gapped in the process, so its topological state before and after WN-annihilation must be the same.

Recently, Refs. [63, 64] showed that s-wave superconductor vortices in Dirac semimetals can trap helical MFs protected by crystal symmetries. Unlike those vortices, the gapless vortex here is a 1D phase of matter rather than a critical point as it cannot be gapped out by perturbatively changing the crystal space group. Ref. [65] found that below a critical doping in a lattice model of a Dirac semimetal with two Dirac nodes, an s-wave vortex normal to the line joining the nodes is gapped and traps a surface MF. The MF survives when the Dirac semimetal is perturbed into a minimal TWSM with four WNs in the plane normal to the vortex, assuming s-wave pairing even with broken inversion symmetry ($\mathcal{I}$) in the TWSM. In comparison, our criteria include the TWSM results of Ref. [65] at low doping, but allow arbitrary numbers and configurations of type-I WNs, trivial Fermi surfaces and filled topological bands in the bulk, FAs, Fermi loops and Dirac nodes on the surface, and arbitrary pairing that opens a full gap when uniform.

Continuum analytics:- Consider a canonical WN of chirality $h = \pm 1$ described by $H_W(\boldsymbol{P}) = h\sum_j v_j \Sigma_j P_j - \mu$, where Σ_j, $j = X, Y, Z$, are Pauli matrices spanning the lowest two bands and $\boldsymbol{P}$ is the momentum relative to the WN. At $P_Z = 0$, H_W resembles the 2D surface Hamiltonian of a 3D topological insulator [3, 5, 6, 66]. If $v_X = v_Y$ and $\mu = 0$, it yields a pseudospin-polarized MF with $\langle \Sigma_Z \rangle = w$ in the core of an s-wave superconductor vortex, $\Delta(\boldsymbol{R}) = \Delta(R)e^{iw\Theta}$, $w = \pm 1$ [5]. Being topologically protected, the MF will survive albeit with partial polarization, $0 < w\langle \Sigma_Z \rangle < 1$, when $v_X \neq v_Y$, $\mu \neq 0$ and the pairing is arbitrary but real and non-zero on the Fermi surface. In fact, the MF only requires a Fermi surface Berry phase of π in the weak-pairing, smooth-vortex limit [6]. When $P_Z \neq 0$, the MF disperses as $E_h = hv_Z P_Z \langle \Sigma_z \rangle$, thus realizing a chiral MF with chirality h at $P_Z = 0$ or the k_z of the parent WN. In a real TWSM, k_z-conservation forbids hybridization between chiral MFs whose parent WNs are at different k_z, resulting in a gapless vortex [Fig. 1(b)].

Next, consider a minimal TWSM with one quadruplet of WNs at $(\pm \boldsymbol{K}_1, 0)$, $(\pm \boldsymbol{K}_2, 0)$, where WNs at $\pm \boldsymbol{K}_n$ are related by $\mathcal{T}$ and have chirality $(-1)^n$. Suppose FAs on the $z = 0$ surface connect $\boldsymbol{K}_1$ to $\boldsymbol{K}_2$ and $-\boldsymbol{K}_1$ to $-\boldsymbol{K}_2$, and Fermi surfaces around the WNs are well-separated. In the presence of a superconductor vortex along $\hat{\mathbf{z}}$, each WN produces a chiral MF dispersing along $(-1)^n \hat{\mathbf{z}}$ with a wavefunction $\psi_{\pm n} = e^{i\boldsymbol{K}_n \cdot \boldsymbol{r}} \varphi_n(\boldsymbol{r})$, where $\varphi_n(\boldsymbol{r})$ is the zero mode of the vortex Hamiltonian near the n^{th} WN. The chiral MFs remain robust when $|\boldsymbol{K}_n \xi| \to \infty$, but hybridize for finite $|\boldsymbol{K}_n \xi|$. Neglecting hybridization between equi-chiral chiral MFs, a generic perturbation H' in the basis $(\psi_{+1}, \psi_{-1}, \psi_{+2}, \psi_{-2})^T$ has the form $H' = \begin{pmatrix} 0 & iQ \\ -iQ^\dagger & 0 \end{pmatrix}$ where $Q = \begin{pmatrix} q_{12} & q_{1\bar{2}} \\ q_{\bar{1}2} & q_{\bar{1}\bar{2}} \end{pmatrix}$ and $q_{mn} =$

$\langle\psi_m|H'|\psi_n\rangle$. If H' preserves $\mathcal{T}$, then $q_{mn} = q_{\bar{m}\bar{n}}$ and the vortex is a gapped 1D superconductor with topological invariant $\nu = \mathrm{sgn}(\mathrm{Pf}[H']) = \mathrm{sgn}(|q_{12}|^2 - |q_{1\bar{2}}|^2)$ [7]. For a spatially smooth perturbation, q_{mn} decays with $|\boldsymbol{K}_m - \boldsymbol{K}_n|$; for instance, band curvature terms yield $q_{mn} \sim e^{-\frac{1}{2}|K_m-K_n|^2\xi/\Delta_0}$ for a linear vortex profile with slope Δ_0/ξ [67]. Then, $|\boldsymbol{K}_1 - \boldsymbol{K}_2| \lesssim |\boldsymbol{K}_1 + \boldsymbol{K}_2|$ produces a trivial vortex while $|\boldsymbol{K}_1 - \boldsymbol{K}_2| \gtrsim |\boldsymbol{K}_1 + \boldsymbol{K}_2|$ yields a topological vortex with end MFs. On the surface, geodesics connecting $\boldsymbol{K}_1$ to $\boldsymbol{K}_2$ and $-\boldsymbol{K}_1$ to $-\boldsymbol{K}_2$, along with the FAs, form $M = 2$ loops. In contrast, geodesics connecting $\boldsymbol{K}_1$ to $-\boldsymbol{K}_2$ and $-\boldsymbol{K}_1$ to $\boldsymbol{K}_2$ form $M = 1$ loops with the FAs. Thus, there is a one-to-one correspondence between ν and M that is captured by (1). The Gaussian form of q_{mn} further ensures only logarithmic corrections to the above inequalities due to $\mathcal{O}(1)$ pre-factors.

Next, consider moving the WNs away from $k_z = 0$ in pairs while preserving $\mathcal{T}$ in the normal state. If $K_{1z} = K_{2z}$, the chiral MF $\psi_{+1}(\boldsymbol{r})$ can hybridize with $\psi_{+2}(\boldsymbol{r})$ but not with $\psi_{-2}(\boldsymbol{r})$, so the resulting vortex is adiabatically connected to the trivial vortex where all WNs are at $k_z = 0$, $q_{12} \neq 0$ and $q_{1\bar{2}} = 0$. In contrast, if $K_{1z} = -K_{2z}$, the adiabatic equivalent with all WNs at $k_z = 0$ has $q_{1\bar{2}} \neq 0$ and $q_{12} = 0$, which is a topological vortex. These conclusions extend straightforwardly to more quadruplets of WNs, thus proving (1) for arbitrary configurations of WNs and FAs.

Finally, let us consider the effects of additional bands on our criteria. A filled topological band will produce a 2D Dirac node or Fermi loop on the surface in the normal state, thereby changing the parity of M. However, the superconductor vortex will trap another surface MF and acquire a bulk gap due to this band, thus preserving (1). Suppose the bulk also contains trivial Fermi surfaces, i.e., Fermi surface that do not enclose WNs or other band intersections. For pairing that is real and non-zero on the Fermi surface, a vortex will contain bands $\varepsilon_n(k_z) \sim \frac{\Delta_0}{\xi l_F(k_z)}\left(n + \frac{1}{2} + \frac{\phi_F(k_z)}{2\pi}\right)$ for each trivial Fermi surface, where $n \in \mathbb{Z}$ and $l_F(k_z)$ ($\phi_F(k_z)$) is the perimeter (Berry phase) of the Fermi surface cross-section at k_z [6]. Unless $\phi_F(k_z) = 0$, trivial Fermi surfaces come in pairs with opposite Berry phases $\pm\phi_F(k_z)$ to ensure that the constant-k_z slice is a sensible 2D metal. As a result, slices with $\phi_F(k_z) \neq \pi$ will acquire a vortex minigap $\sim \Delta_0/\xi l_F(k_z)$ while slices with $\phi_F(k_z) = \pm\pi$, where the minigap vanishes, will host counter-propagating chiral MFs that will generically hybridize and gap out. In summary, additional bands will not interconvert gapped and gapless vortices and filled bands always preserve our general criteria.

For gapped vortices, predicted to obey (1), curable violations due to trivial Fermi surfaces occur in two cases: (i) a surface Fermi loop or Dirac node gets buried under the surface projection of a bulk Fermi surface, resulting in $M_{\text{observable}} = M - 1$. This can be cured in principle by doping to expose the relevant surface state; (ii) a Fermi surface centered at $k_z = 0$ or π is past the doping threshold for a vortex phase transition [6], which changes the vortex phase without changing M. This can be fixed by noting that such a Fermi surface has a pair of slices away from $k_z = 0, \pi$ where $\phi_F(k_z) = \pi$. An incurable violation occurs when $\phi_F(k_z) = \pi$ at the precise k_z where a WN exists, the WN is closer to the trivial Fermi surface than to other anti-chiral WNs at the same k_z *and* the chiral MFs produced by the trivial Fermi surface and the WN have opposite chiralities. Then, H' must include hybridization between these MFs, but (1) is ruined because M stays unchanged.

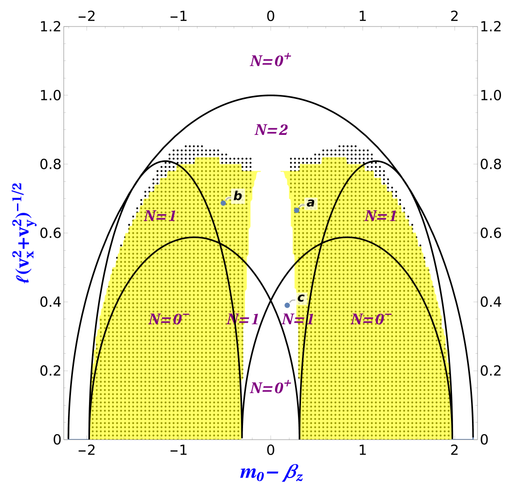

Figure 2. Vortex topological phases predicted by (1) and computed numerically. The yellow mask (black dots) denote a vortex predicted (computed) to be topological. Black lines separate the normal states: TWSMs with $N = 1, 2$ quadruplets of WNs at $k_z = 0$ and trivial/topological ($N = 0^{\pm}$) insulators. We fix $v_{x,y} = 1.18, .856$, $\beta_{x,y,z} = .856, 1.178, 3.0$, $\Delta(r) = 0.42\tanh(0.3r)$ and $L_{x,y} = 31$. Points **t**, **m** and **b** are further studied in Fig. 3

Lattice numerics:- We support our general claims with numerics on an orthorhombic lattice model defined by $H(\boldsymbol{k}) = \tau_x\boldsymbol{\sigma}\cdot\boldsymbol{d}(\boldsymbol{k}) + \tau_z m(\boldsymbol{k}) - \tau_y\sigma_z\ell$ where $d_i = v_i \sin k_i$, $i = x, y, z$, $m(\boldsymbol{k}) = m_0 - \sum_i \beta_i \cos k_i$ and τ_i (σ_i) are Pauli matrices in orbital (spin) space. Varying $\beta_{x,y,z}$ and ℓ allows tuning into trivial and topological insulating phases as well as TWSMs with up to two quadruplets of WNs each at $k_z = 0, \pi$ at the Fermi level. We then introduce an s-wave superconductor vortex $\Delta(\boldsymbol{r}) = |\Delta(r)|e^{i\theta}$ and diagonalize the Bogoliubov-deGennes Hamiltonian in 2D real space at fixed k_z to obtain the spectrum and the topological invariant [7] for a class D 1D superconductor [61, 62]. In [68], we describe graphical methods for determining the normal state of $H(\boldsymbol{k})$ and FA-configuration as well as further details of the lattice numerics. Fig. 2 shows that the prediction using (1) agrees excellently with the explicit calculation. We found smaller mismatch for larger systems or weaker pairing, suggesting that it is due to departure from the thermodynamic and weak-pairing limits.

Fig. 3 shows the Fermi-geodesic loops in the normal state and the probability density of the lowest few vortex

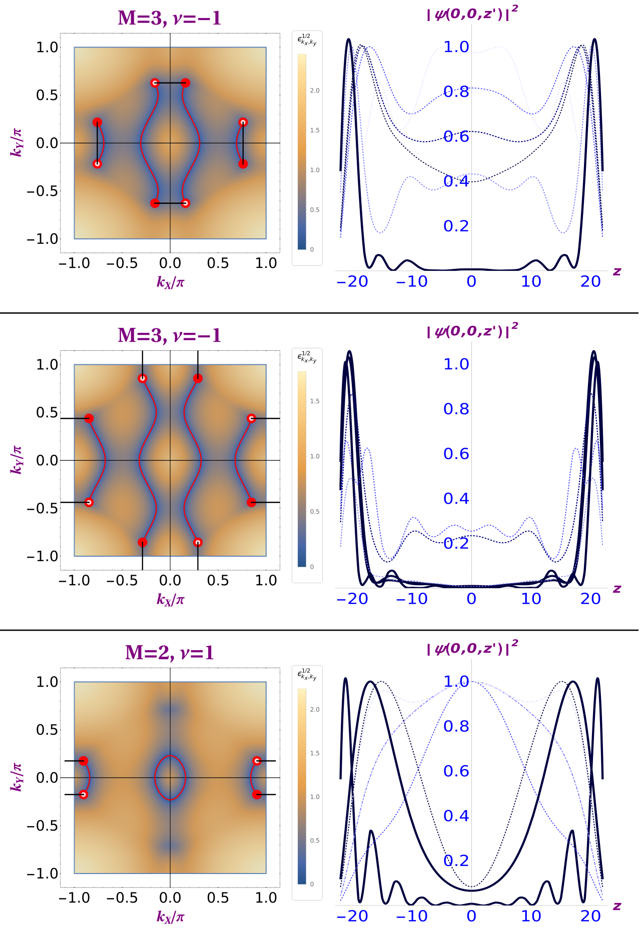

Figure 3. Left column: Color plots of the lowest band for a 45-layer slab in the normal state for the points **t**, **m** and **b** in Fig. 2 defined by $l = 0.942, m_0 = 6.28$ (top), $l = 0.972$, $m_0 = 5.48$ (middle) and $l = 0.552$, $m_0 = 6.18$ (bottom). Red filled (empty) circles denote surface projections of right-(left-)handed WNs. Surface projections of geodesics (black lines) connecting anti-chiral WNs at $k_z = 0$ form M closed loops along with the FAs (red curves). Right column: Probability densities of six lowest energy states along a z-oriented vortex in a $31\times31\times45$-site system. Bold and dotted lines mark states with energies $E < 5.0\times10^{-3}$, considered "zero energy", and $E > 1.0\times10^{-2}$.

modes for select points in Fig. 2. The FAs are obtained by plotting the lowest energy at each surface momentum in the normal phase and the geodesics are simply straight lines connecting proximate anti-chiral WNs at $k_z = 0$. The probability densities are computed by diagonalizing the vortex Hamiltonian in 3D real space. For each selected point, we find that the number of MFs localized to the vortex ends equals M. In Fig. 4, we show that tilting the vortex drives phase transitions between trivial, topological and gapless vortices since geodesics connect WNs at the same k_z. The transitions are expected at infinitesimal tilting in the weak-pairing, smooth-vortex limit, while the numerics find the transitions to occur at small angles.

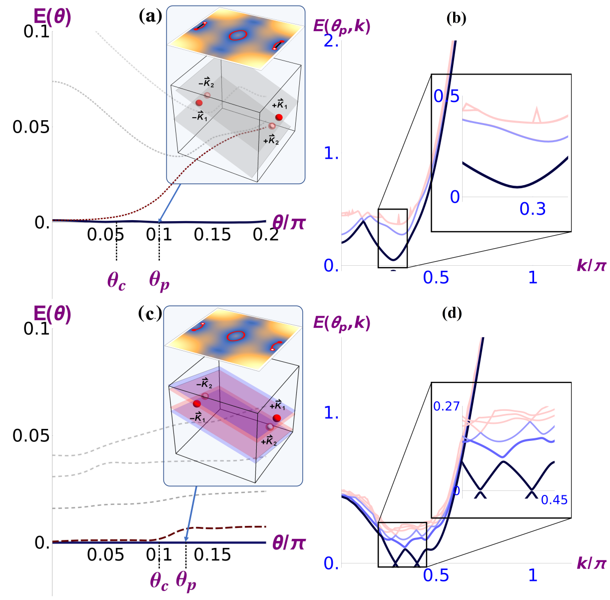

Figure 4. Topological phase transitions upon tilting the $M = 2$ trivial vortex in Fig. 3 (bottom) obtained by diagonalization in real-space (a, c) and k-space (b, d). (a) Tilting about the x-axis produces $M = 3$ (inset) and gaps out one of the two MFs at $\theta_c \approx 0.06\pi$. (b) At $\theta_p = 0.1\pi$, the bulk vortex is gapped, so the surviving MF in (a) at $\theta > \theta_c$ is protected and the vortex is topological. (c, d) Analogous figures for tilting about $x + y = z = 0$. In (c), a small gap opens for one MF at $\theta_c \approx 0.1\pi$ while the surface has open Fermi-geodesic arcs (inset). (d) The bulk vortex is gapless, indicating that the gap in (c) is a finite size gap.

Candidate material:- We propose $Li(Fe_{0.91}Co_{0.09})As$ and $Fe_{1+y}Se_{0.45}Te_{0.55}$ with broken $\mathcal{I}$ as candidate materials. $Li(Fe_{0.91}Co_{0.09})As$ is a Dirac semimetal with two Dirac nodes on the c-axis of the crystal [69] and shows strongly type-II superconductivity below $T_c \approx 9K$ [70]. $FeSe_{0.45}Te_{0.55}$ realizes a doped topological insulator that turns into a type-II superconductor below $T_c \approx 14.5K$ [25, 26], but the normal state also has two Dirac nodes along the c-axis $\sim 15meV$ above the Fermi level that may be accessed with naturally occurring Fe-dopants [69]. Perturbatively breaking $\mathcal{I}$ while preserving $\mathcal{T}$ will turn the Dirac semimetals into a TWSM with four WNs at $\pm\boldsymbol{K}_1, \pm\boldsymbol{K}_2$ with $K_1^c \approx K_2^c \gg |\boldsymbol{K}_1 - \boldsymbol{K}_2|$. If superconductivity survives $\mathcal{I}$-breaking, a vortex along $\hat{\mathbf{z}}$ will be topological (trivial) according to (1) if $|K_{1z}| = |K_{2z}|$ and $(\hat{\mathbf{z}} \times \boldsymbol{K}_1)\cdot(\hat{\mathbf{z}} \times \boldsymbol{K}_2) > 0$ (< 0), whereas a vortex in any other direction will be gapless. Assuming typical values $v \sim 10^5 m/s$ for the Dirac velocity, chemical potential $\mu \sim 100K$ relative to the WNs, $\Delta_0 \sim 5K$, $\xi \sim 5nm \ll$ the penetration depth $d \sim 10^2 nm$ observed in LiFeAs [64] which guarantees negligible intervortex tunneling ($\propto e^{-d/\xi}$), and $|\boldsymbol{K}_1 - \boldsymbol{K}_2|/K_1^c \approx 0.1$, we estimate a vortex gap of $\sim 0.1K$. However, the gap depends exponentially on ξ, $|\boldsymbol{K}_1 - \boldsymbol{K}_2|$ and Δ_0, so it will change substantially for small changes in their values [71].

We acknowledge financial support from the Department of Physics and the College of Natural Sciences and Mathematics, University of Houston and NSF-DMR-2047193.

[1] Jason Alicea. New directions in the pursuit of majorana fermions in solid state systems. *Reports on Progress in Physics*, 75(7), 2012. ISSN 00344885. doi:10.1088/0034-4885/75/7/076501. URL https://iopscience.iop.org/article/10.1088/0034-4885/75/7/076501. (document)

[2] Andreas Aste. A direct road to majorana fields. *Symmetry*, 2(4):1776–1809, 2010. ISSN 20738994. doi:10.3390/sym2041776. URL https://doi.org/10.3390/sym2041776.

[3] C.W.J. Beenakker. Search for majorana fermions in superconductors. *Annual Review of Condensed Matter Physics*, 4(1):113–136, 2013. ISSN 1947-5454. doi:10.1146/annurev-conmatphys-030212-184337. URL https://doi.org/10.1146/annurev-conmatphys-030212-184337. (document)

[4] Steven R. Elliott and Marcel Franz. Colloquium: Majorana fermions in nuclear, particle, and solid-state physics. *Reviews of Modern Physics*, 87(1), 2015. ISSN 15390756. doi:10.1103/RevModPhys.87.137. URL https://doi.org/10.1103/RevModPhys.87.137.

[5] Liang Fu and C. L. Kane. Superconducting proximity effect and majorana fermions at the surface of a topological insulator. *Physical Review Letters*, 100(9):96407, 2008. ISSN 00319007. doi:10.1103/PhysRevLett.100.096407. URL https://doi.org/10.1103/PhysRevLett.100.096407. (document)

[6] Pavan Hosur, Pouyan Ghaemi, Roger S. K. Mong, and Ashvin Vishwanath. Majorana modes at the ends of superconductor vortices in doped topological insulators. *Physics Review Letters*, 107:097001, Aug 2011. doi:10.1103/PhysRevLett.107.097001. URL https://link.aps.org/doi/10.1103/PhysRevLett.107.097001. (document)

[7] A Yu Kitaev. Unpaired majorana fermions in quantum wires. *Physics-Uspekhi*, 44(10S):131–136, Oct 2001. doi:10.1070/1063-7869/44/10s/s29. URL https://doi.org/10.10702F1063-78692F442F10s2Fs29. (document)

[8] Martin Leijnse and Karsten Flensberg. Introduction to topological superconductivity and majorana fermions. *Semiconductor Science and Technology*, 27(12), 2012. ISSN 02681242. doi:10.1088/0268-1242/27/12/124003.

[9] Qin Liu, Chen Chen, Tong Zhang, Rui Peng, Ya Jun Yan, Chen Hao Ping Wen, Xia Lou, Yu Long Huang, Jin Peng Tian, Xiao Li Dong, Guang Wei Wang, Wei Cheng Bao, Qiang Hua Wang, Zhi Ping Yin, Zhong Xian Zhao, and Dong Lai Feng. Robust and clean majorana zero mode in the vortex core of high-temperature superconductor (li0.84fe0.16)ohfese. *Physical Review X*, 8(4):41056, 2018. ISSN 21603308. doi:10.1103/PhysRevX.8.041056. URL https://doi.org/10.1103/PhysRevX.8.041056.

[10] Xiao Ping Liu, Yuan Zhou, Yi Fei Wang, and Chang De Gong. Characterizations of topological superconductors: Chern numbers, edge states and majorana zero modes. *New Journal of Physics*, 19(9), 2017. ISSN 13672630. doi:10.1088/1367-2630/aa8022. URL https://doi.org/10.1088/1367-2630/aa8022.

[11] Roman M. Lutchyn, Tudor D. Stanescu, and S. Das Sarma. Search for majorana fermions in multiband semiconducting nanowires. *Physical Review Letters*, 106(12):1–4, 2011. ISSN 00319007. doi:10.1103/PhysRevLett.106.127001. URL https://doi.org/10.1103/PhysRevLett.106.127001. (document)

[12] Ning Ma. Majorana fermions in condensed matter: An outlook. *Physica B: Condensed Matter*, 512(January):100–101, 2017. ISSN 09214526. doi:10.1016/j.physb.2017.01.028. URL https://doi.org/10.1016/j.physb.2017.01.028.

[13] N. Mohanta and A. Taraphder. Topological superconductivity and majorana bound states at the $\mathrm{LaAlO_3/SrTiO_3}$ interface. *Epl*, 108(6), 2014. ISSN 12864854. doi:10.1209/0295-5075/108/60001. URL https://doi.org/10.1209/0295-5075/108/60001.

[14] V. Mourik, K. Zuo, S. M. Frolov, S. R. Plissard, E. P.A.M. Bakkers, and L. P. Kouwenhoven. Signatures of majorana fermions in hybrid superconductor-semiconductor nanowire devices. *Science*, 336(6084):1003–1007, 2012. ISSN 10959203. doi:10.1126/science.1222360. URL https://doi.org/10.1126/science.1222360. (document)

[15] Stevan Nadj-Perge, Ilya K. Drozdov, Jian Li, Hua Chen, Sangjun Jeon, Jungpil Seo, Allan H. MacDonald, B. Andrei Bernevig, and Ali Yazdani. Observation of majorana fermions in ferromagnetic atomic chains on a superconductor. *Science*, 346(6209):602–607, 2014. ISSN 10959203. doi:10.1126/science.1259327. URL https://doi.org/10.1126/science.1259327.

[16] Xiao Liang Qi and Shou Cheng Zhang. Topological insulators and superconductors. *Reviews of Modern Physics*, 83(4), 2011. ISSN 00346861. doi:10.1103/RevModPhys.83.1057. URL https://doi.org/10.1103/RevModPhys.83.1057.

[17] N. Read and Dmitry Green. Paired states of fermions in two dimensions with breaking of parity and time-reversal symmetries and the fractional quantum hall effect. *Physical Review B - Condensed Matter and Materials Physics*, 2000. ISSN 1550235X. doi:10.1103/PhysRevB.61.10267. URL https://doi.org/10.1103/PhysRevB.61.10267. (document)

[18] Leonid P. Rokhinson, Xinyu Liu, and Jacek K. Furdyna. The fractional a.c. josephson effect in a semiconductor-superconductor nanowire as a signature of majorana particles. *Nature Physics*, 8(11):795–799, 2012. ISSN 17452481. doi:10.1038/nphys2429. URL http://dx.doi.org/10.1038/nphys2429.

[19] Masatoshi Sato and Satoshi Fujimoto. Existence of majorana fermions and topological order in nodal superconductors with spin-orbit interactions in external magnetic fields. *Physical Review Letters*, 105(21):1–4, 2010. ISSN 00319007. doi:10.1103/PhysRevLett.105.217001. URL https://doi.org/10.1103/PhysRevLett.105.217001.

[20] Masatoshi Sato and Yoichi Ando. Topological superconductors: A review. *Reports on Progress in Physics*, 80(7):1–45, 2017. ISSN 00344885. doi:10.1088/1361-6633/aa6ac7. URL https://doi.org/10.1088/1361-6633/aa6ac7. (document)

[21] Tudor D. Stanescu, Jay D. Sau, Roman M. Lutchyn, and S. Das Sarma. Proximity effect at the superconductor-topological insulator interface. *Physical Review B - Condensed Matter and Materials Physics*, 2010. ISSN 10980121. doi:10.1103/PhysRevB.81.241310. URL https://doi.org/10.1103/PhysRevB.81.241310. (document)

[22] Gang Xu, Biao Lian, Peizhe Tang, Xiao-Liang Qi, and Shou-Cheng Zhang. Topological superconductivity on the surface of fe-based superconductors. *Physical Review Letters*, 117:047001, Jul 2016. doi:10.1103/PhysRevLett.117.047001. URL https://link.aps.org/doi/10.1103/PhysRevLett.117.047001. (document)

[23] T. Machida, Y. Sun, S. Pyon, S. Takeda, Y. Kohsaka, T. Hanaguri, T. Sasagawa, and T. Tamegai. Zero-energy vortex bound state in the superconducting topological surface state of fe(se,te). *Nature Materials*, 18(8):811–815, 2019. doi:10.1038/s41563-019-0397-1. URL https://doi.org/10.1038/s41563-019-0397-1.

[24] Lingyuan Kong, Shiyu Zhu, Michał Papaj, Hui Chen, Lu Cao, Hiroki Isobe, Yuqing Xing, Wenyao Liu, Dongfei Wang, Peng Fan, Yujie Sun, Shixuan Du, John Schneeloch, Ruidan Zhong, Genda Gu, Liang Fu, Hong-Jun Gao, and Hong Ding. Half-integer level shift of vortex bound states in an iron-based superconductor. *Nature Physics*, 15(11):1181–1187, 2019. doi:10.1038/s41567-019-0630-5. URL https://doi.org/10.1038/s41567-019-0630-5.

[25] Dongfei Wang, Lingyuan Kong, Peng Fan, Hui Chen, Shiyu Zhu, Wenyao Liu, Lu Cao, Yujie Sun, Shixuan Du, John Schneeloch, Ruidan Zhong, Genda Gu, Liang Fu, Hong Ding, and Hong-Jun Gao. Evidence for majorana bound states in an iron-based superconductor. *Science (New York, N.Y.)*, 2018. ISSN 1095-9203. doi:10.1126/science.aao1797. URL https://doi.org/10.1126/science.aao1797. (document)

[26] Peng Zhang, Peng Zhang, Koichiro Yaji, Takahiro Hashimoto, Yuichi Ota, Takeshi Kondo, Kozo Okazaki, Zhijun Wang, Jinsheng Wen, G. D. Gu, Hong Ding, Shik Shin, Peng Zhang, Koichiro Yaji, Takahiro Hashimoto, Yuichi Ota, Takeshi Kondo, Kozo Okazaki, Zhijun Wang, Jinsheng Wen, G. D. Gu, Hong Ding, and Shik Shin. Observation of topological superconductivity on the surface of an iron-based superconductor. *Science*, 360(April):182, 2018. ISSN 10959203. doi:10.1126/science.aan4596. URL https://doi.org/10.1126/science.aan4596. (document)

[27] Conyers Herring. Accidental degeneracy in the energy bands of crystals. *Phys. Rev.*, 52:365–373, Aug 1937. doi:10.1103/PhysRev.52.365. URL https://link.aps.org/doi/10.1103/PhysRev.52.365. (document)

[28] G.E. Volovik. *The Universe in a Helium Droplet*. International Series of Monographs on Physics. OUP Oxford, 2009. ISBN 9780199564842. URL https://books.google.com/books?id=6uj76kFJOHEC.

[29] Xiangang Wan, Ari M. Turner, Ashvin Vishwanath, and Sergey Y. Savrasov. Topological semimetal and fermi-arc surface states in the electronic structure of pyrochlore iridates. *Physical Review B*, 83:205101, May 2011. doi:10.1103/PhysRevB.83.205101. URL https://link.aps.org/doi/10.1103/PhysRevB.83.205101.

[30] N. P. Armitage, E. J. Mele, and Ashvin Vishwanath. Weyl and dirac semimetals in three-dimensional solids. *Reviews of Modern Physics*, 2018. ISSN 15390756. doi:10.1103/RevModPhys.90.015001. URL https://doi.org/10.1103/RevModPhys.90.015001. (document)

[31] P. Hosur and X. Qi. Recent developments in transport phenomena in Weyl semimetals. *Comptes Rendus Physique*, 14(9-10), 2013. ISSN 16310705. doi:10.1016/j.crhy.2013.10.010. URL https://doi.org/10.1016/j.crhy.2013.10.010. (document)

[32] A. A. Burkov. Anomalous hall effect in weyl metals. *Physical Review Letters*, 113:187202, Oct 2014. doi:10.1103/PhysRevLett.113.187202. URL https://link.aps.org/doi/10.1103/PhysRevLett.113.187202.

[33] A A Burkov. Weyl Metals. *Annual Review of Condensed Matter Physics*, 9(1):359–378, 2018. ISSN 1947-5454. doi:10.1146/annurev-conmatphys-033117-054129. URL https://doi.org/10.1146/annurev-conmatphys-033117-054129.

[34] A A Burkov. Chiral anomaly and transport in Weyl metals. *Journal of Physics: Condensed Matter*, 27(11):113201, feb 2015. doi:10.1088/0953-8984/27/11/113201. URL https://doi.org/10.1088/2F0953-8984/2F27/2F11/2F113201.

[35] Y Chen, Si Wu, and A A Burkov. Axion response in Weyl semimetals. *Physical Review B*, 88(12):125105, sep 2013. doi:10.1103/PhysRevB.88.125105. URL http://link.aps.org/doi/10.1103/PhysRevB.88.125105.

[36] A A Zyuzin and A A Burkov. Topological response in Weyl semimetals and the chiral anomaly. *Physical Review B*, 86(11):115133, sep 2012. doi:10.1103/PhysRevB.86.115133. URL http://link.aps.org/doi/10.1103/PhysRevB.86.115133.

[37] P. Hosur and X.-L. Qi. Tunable circular dichroism due to the chiral anomaly in Weyl semimetals. *Physical Review B - Condensed Matter and Materials Physics*, 91(8), 2015. ISSN 1550235X. doi:10.1103/PhysRevB.91.081106. URL https://doi.org/10.1103/PhysRevB.91.081106.

[38] Jin Hu, Su-Yang Xu, Ni Ni, and Zhiqiang Mao. Transport of Topological Semimetals. *Annual Review of Materials Research*, 49(1):207–252, 2019. doi:10.1146/annurev-matsci-070218-010023. URL https://doi.org/10.1146/annurev-matsci-070218-010023.

[39] Fernando de Juan, Adolfo G Grushin, Takahiro Morimoto, and Joel E Moore. Quantized circular photogalvanic effect in Weyl semimetals. *Nature Communications*, 8(1):15995, 2017. doi:10.1038/ncomms15995. URL https://doi.org/10.1038/ncomms15995.

[40] Takuro Kobayashi, Taiki Matsushita, Takeshi Mizushima, Atsushi Tsuruta, and Satoshi Fujimoto. Negative Thermal Magnetoresistivity as a Signature of a Chiral Anomaly in Weyl Superconductors. *Physical Review Letters*, 121(20):207002, 2018. ISSN 10797114. doi:

10.1103/PhysRevLett.121.207002. URL https://doi.org/10.1103/PhysRevLett.121.207002.

[41] Karl Landsteiner. Anomalous transport of Weyl fermions in Weyl semimetals. *Physical Review B*, 89 (7):75124, feb 2014. doi:10.1103/PhysRevB.89.075124. URL http://link.aps.org/doi/10.1103/PhysRevB.89.075124.

[42] Hailong Li, Haiwen Liu, Hua Jiang, and X. C. Xie. 3d quantum hall effect and a global picture of edge states in weyl semimetals. *Phys. Rev. Lett.*, 125: 036602, Jul 2020. doi:10.1103/PhysRevLett.125.036602. URL https://link.aps.org/doi/10.1103/PhysRevLett.125.036602.

[43] R Loganayagam and Piotr Surówka. Anomaly/transport in an Ideal Weyl gas. *Journal of High Energy Physics*, 2012(4):97, apr 2012. ISSN 1029-8479. doi: 10.1007/JHEP04(2012)097. URL https://doi.org/10.1007/JHEP04(2012)097.

[44] Naoto Nagaosa, Takahiro Morimoto, and Yoshinori Tokura. Transport, magnetic and optical properties of Weyl materials. *Nature Reviews Materials*, 5(8):621–636, 2020. doi: 10.1038/s41578-020-0208-y. URL https://doi.org/10.1038/s41578-020-0208-y.

[45] Anna Corinna Niemann, Johannes Gooth, Shu Chun Wu, Svenja Bäßler, Philip Sergelius, Ruben Hühne, Bernd Rellinghaus, Chandra Shekhar, Vicky Süß, Marcus Schmidt, Claudia Felser, Binghai Yan, and Kornelius Nielsch. Chiral magnetoresistance in the Weyl semimetal NbP. *Scientific Reports*, 7(November 2016):3–8, 2017. ISSN 20452322. doi:10.1038/srep43394. URL http://dx.doi.org/10.1038/srep43394. (document)

[46] Pallab Goswami, Girish Sharma, and Sumanta Tewari. Optical activity as a test for dynamic chiral magnetic effect of Weyl semimetals. *Physical Review B*, 92(16): 161110, oct 2015. doi:10.1103/PhysRevB.92.161110. URL https://link.aps.org/doi/10.1103/PhysRevB.92.161110.

[47] Chao-Xing Liu, Peng Ye, and Xiao-Liang Qi. Chiral gauge field and axial anomaly in a Weyl semimetal. *Physical Review B*, 87(23):235306, jun 2013. doi: 10.1103/PhysRevB.87.235306. URL http://link.aps.org/doi/10.1103/PhysRevB.87.235306.

[48] K.-Y. Yang, Y.-M. Lu, and Y Ran. Quantum Hall effects in a Weyl semimetal: Possible application in pyrochlore iridates. *Physical Review B*, 84(7):75129, aug 2011. doi:10.1103/PhysRevB.84.075129. URL https://doi.org/10.1103/PhysRevB.84.075129.

[49] Chandra Shekhar, Ajaya K Nayak, Yan Sun, Marcus Schmidt, Michael Nicklas, Inge Leermakers, Uli Zeitler, Yurii Skourski, Jochen Wosnitza, Zhongkai Liu, Yulin Chen, Walter Schnelle, Horst Borrmann, Yuri Grin, Claudia Felser, and Binghai Yan. Extremely large magnetoresistance and ultrahigh mobility in the topological Weyl semimetal candidate NbP. *Nature Physics*, 11(8):645–649, 2015. doi:10.1038/nphys3372. URL https://doi.org/10.1038/nphys3372.

[50] Kabyashree Sonowal, Ashutosh Singh, and Amit Agarwal. Giant optical activity and kerr effect in type-i and type-ii weyl semimetals. *Phys. Rev. B*, 100: 085436, Aug 2019. doi:10.1103/PhysRevB.100.085436. URL https://link.aps.org/doi/10.1103/PhysRevB.100.085436.

[51] D T Son and B Z Spivak. Chiral anomaly and classical negative magnetoresistance of Weyl metals. *Physical Review B*, 88(10):104412, sep 2013. doi: 10.1103/PhysRevB.88.104412. URL http://link.aps.org/doi/10.1103/PhysRevB.88.104412.

[52] C J Tabert, J P Carbotte, and E J Nicol. Optical and transport properties in three-dimensional Dirac and Weyl semimetals. *Physical Review B*, 93(8), 2016. ISSN 24699969. doi:10.1103/PhysRevB.93.085426. URL https://doi.org/10.1103/PhysRevB.93.085426.

[53] M M Vazifeh and M Franz. Electromagnetic Response of Weyl Semimetals. *Physical Review Letters*, 111(2): 27201, jul 2013. doi:10.1103/PhysRevLett.111.027201. URL http://link.aps.org/doi/10.1103/PhysRevLett.111.027201.

[54] Shuo Wang, Ben Chuan Lin, An Qi Wang, Da Peng Yu, and Zhi Min Liao. Quantum transport in Dirac and Weyl semimetals: a review. *Advances in Physics: X*, 2(3):518–544, 2017. ISSN 23746149. doi: 10.1080/23746149.2017.1327329. URL http://dx.doi.org/10.1080/23746149.2017.1327329.

[55] Huichao Wang and Jian Wang. Electron transport in Dirac and Weyl semimetals. *Chinese Physics B*, 27(10):107402, oct 2018. doi:10.1088/1674-1056/27/10/107402. URL https://doi.org/10.1088/2F1674-1056/2F27/2F10/2F107402.

[56] Min Lv and Shou-Cheng Zhang. Dielectric Function, Friedel Oscillation and Plasmons in Weyl Semimetals. *International Journal of Modern Physics B*, 27(25):1350177, 2013. doi:10.1142/S0217979213501774. URL https://doi.org/10.1142/S0217979213501774.

[57] H B Nielsen and M Ninomiya. The Adler-Bell-Jackiw anomaly and Weyl fermions in a crystal. *Physics Letters B*, 130(6):389–396, 1983. ISSN 0370-2693. doi: 10.1016/0370-2693(83)91529-0. URL https://doi.org/10.1016/0370-2693(83)91529-0. (document)

[58] Lijun Meng, Jiafang Wu, Jianxin Zhong, and Rudolf A. Romer. A type of robust superlattice type-i weyl semimetal with four weyl nodes. *Nanoscale*, 11:18358–18366, 2019. doi:10.1039/C9NR04551A. URL http://dx.doi.org/10.1039/C9NR04551A. (document)

[59] Hongming Weng, Chen Fang, Zhong Fang, B Andrei Bernevig, and Xi Dai. Weyl Semimetal Phase in Noncentrosymmetric Transition-Metal Monophosphides. *Physical Review X*, 5(1):11029, mar 2015. doi: 10.1103/PhysRevX.5.011029. URL https://link.aps.org/doi/10.1103/PhysRevX.5.011029.

[60] Jianpeng Liu and David Vanderbilt. Weyl semimetals from noncentrosymmetric topological insulators. *Physical Review B*, 155316(September):1–10, 2014. doi: 10.1103/PhysRevB.90.155316. URL https://doi.org/10.1103/PhysRevB.90.155316. (document)

[61] Shinsei Ryu, Andreas P. Schnyder, Akira Furusaki, and Andreas W.W. Ludwig. Topological insulators and superconductors: Tenfold way and dimensional hierarchy. *New Journal of Physics*, 12, 2010. ISSN 13672630. doi: 10.1088/1367-2630/12/6/065010. URL https://doi.org/10.1088/1367-2630/12/6/065010. (document)

[62] Andreas P. Schnyder, Shinsei Ryu, Akira Furusaki, and Andreas W.W. Ludwig. Classification of topological insulators and superconductors. *AIP Conference Proceedings*, 1134:10–21, 2009. ISSN 0094243X. doi: 10.1063/1.3149481. URL https://doi.org/10.1063/1.3149481. (document)

[63] Elio J. Konig and Piers Coleman. Crystalline-symmetry-protected helical majorana modes in the iron pnictides. *Physical Review Letters*, 122(20), 2019. ISSN 10797114. doi:10.1103/PhysRevLett.122.207001. URL https://doi.org/10.1103/PhysRevLett.122.207001. (document)

[64] Shengshan Qin, Lunhui Hu, Congcong Le, Jinfeng Zeng, Fu-chun Zhang, Chen Fang, and Jiangping Hu. Quasi-1d topological nodal vortex line phase in doped superconducting 3d dirac semimetals. *Physical Review Letters*, 123: 027003, Jul 2019. doi:10.1103/PhysRevLett.123.027003. URL https://link.aps.org/doi/10.1103/PhysRevLett.123.027003. (document)

[65] Zhongbo Yan, Zhigang Wu, and Wen Huang. Vortex end majorana zero modes in superconducting dirac and weyl semimetals. *Phys. Rev. Lett.*, 124:257001, Jun 2020. doi:10.1103/PhysRevLett.124.257001. URL https://link.aps.org/doi/10.1103/PhysRevLett.124.257001. (document)

[66] A. A. Burkov and Leon Balents. Weyl semimetal in a topological insulator multilayer. *Physical Review Letters*, 107(12):1–4, 2011. ISSN 00319007. doi: 10.1103/PhysRevLett.107.127205. URL https://doi.org/10.1103/PhysRevLett.107.127205. (document)

[67] See supplemental material at http://link.aps.org/supplemental for hybridization of chiral majorana fermions which includes refs. [5, 6, 17], . (document)

[68] See supplemental material at http://link.aps.org/supplemental for graphical methods for determining the normal state which includes ref. [72], . (document)

[69] Peng Zhang, Zhijun Wang, Xianxin Wu, Koichiro Yaji, Yukiaki Ishida, Yoshimitsu Kohama, Guangyang Dai, Yue Sun, Cedric Bareille, Kenta Kuroda, Takeshi Kondo, Kozo Okazaki, Koichi Kindo, Xiancheng Wang, Changqing Jin, Jiangping Hu, Ronny Thomale, Kazuki Sumida, Shilong Wu, Koji Miyamoto, Taichi Okuda, Hong Ding, G. D. Gu, Tsuyoshi Tamegai, Takuto Kawakami, Masatoshi Sato, and Shik Shin. Multiple topological states in iron-based superconductors. *Nature Physics*, 15(1):41–47, 2019. doi: 10.1038/s41567-018-0280-z. URL https://doi.org/10.1038/s41567-018-0280-z. (document)

[70] Y. M. Dai, H. Miao, L. Y. Xing, X. C. Wang, P. S. Wang, H. Xiao, T. Qian, P. Richard, X. G. Qiu, W. Yu, C. Q. Jin, Z. Wang, P. D. Johnson, C. C. Homes, and H. Ding. Spin-fluctuation-induced non-fermi-liquid behavior with suppressed superconductivity in $\mathrm{LiFe}_{1-x}\mathrm{Co}_x\mathrm{As}$. *Phys. Rev. X*, 5:031035, Sep 2015. doi:10.1103/PhysRevX.5.031035. URL https://link.aps.org/doi/10.1103/PhysRevX.5.031035. (document)

[71] See supplemental material at http://link.aps.org/supplemental for hybridization gap and calculation of the topological invariant which includes ref. [7], . (document)

[72] Liang Fu, C L Kane, and E J Mele. Topological Insulators in Three Dimensions. *Physical Review Letters*, 98(10): 106803, mar 2007. doi:10.1103/PhysRevLett.98.106803. URL https://link.aps.org/doi/10.1103/PhysRevLett.98.106803. (document)